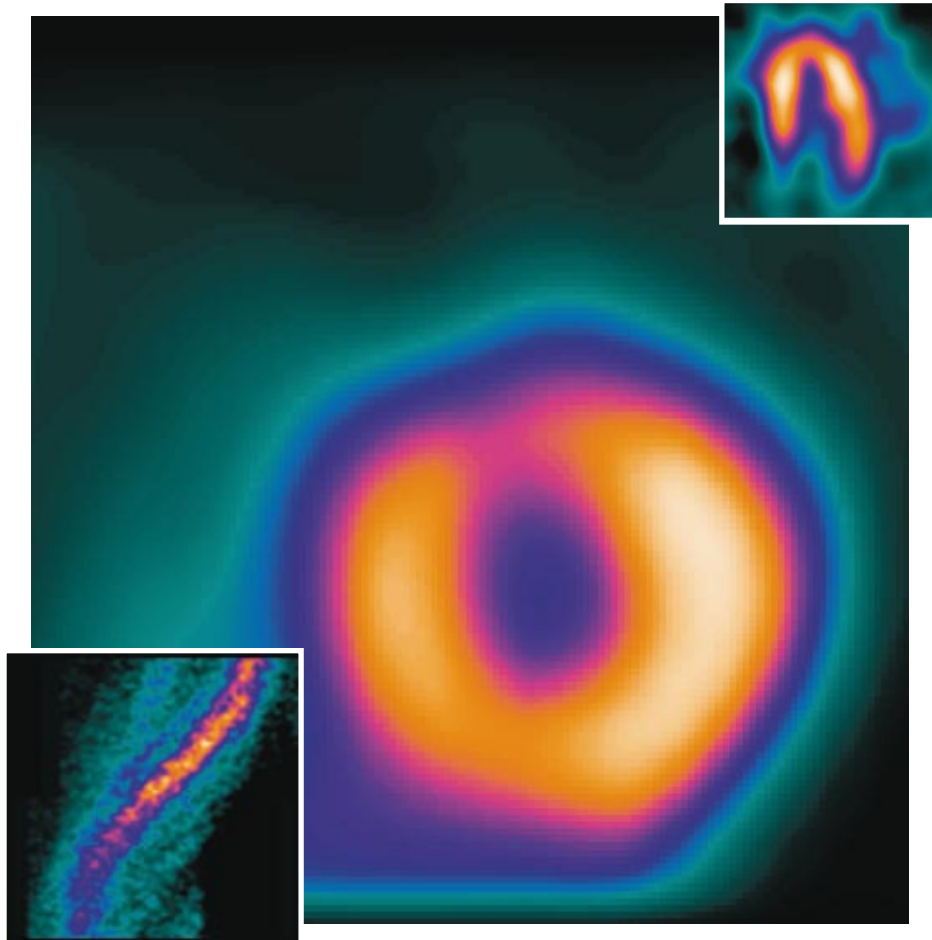


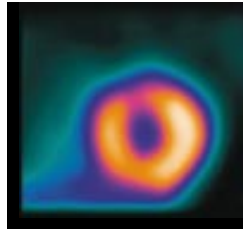
# ATTENUATION CORRECTION



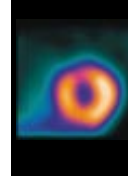
***GE Medical Systems***

---

# Table of Contents



Why Attenuation Correction? .....	3
Transmission Scanning.....	4
Transmission Scan Hardware.....	4
Transmission Scan Mask.....	6
Transmission Scan Dosimetry .....	7
Transmission/Emission Acquisitions .....	8
Sequential Emission/Transmission Scanning .....	9
Simultaneous Interleaved Emission/Transmission Scanning	10
Reconstruction Methods & Attenuation Correction.....	12
Attenuation Correction Methods .....	12
Attenuation Correction with Direct Reconstruction.....	12
Measured Attenuation Correction .....	12
Attenuation Map Reconstruction .....	12
Crosstalk Correction .....	12
Source Flux Correction .....	13
Map Reconstruction .....	13
Emission Pre-processing .....	13
Attenuation Map Scaling.....	13
Scatter Correction .....	13
Uniformity Correction.....	13
Iterative Reconstruction Processing .....	14
Iterative Reconstruction Algorithms .....	15
MLEM .....	15
OSEM .....	15
Emission Post-processing.....	15
Additional Considerations .....	16
Reconstruction Time of Iterative Algorithms .....	16
Other Iterative Attenuation Methods.....	16
Limitations of Iterative Reconstruction .....	16
Results.....	17
Image Data .....	18
References .....	19



## WHY ATTENUATION CORRECTION?

Attenuation correction is aimed at providing improved quantification of tomographic myocardial images, by measuring and correcting for the attenuation from tissue surrounding the myocardium [1, 2]. Attenuation correction has been initially proven on the Optima NX.

Myocardial imaging with thallium-201 and technetium-99m is susceptible to artifacts caused by attenuation of the low energy (72 keV & 140 keV) gamma rays emitted from the patient. Decreased image activity in the anterior and upper septal walls can be caused by increased breast attenuation. Also, decreased image activity in the inferior wall can be produced by diaphragmatic attenuation [3]. Attenuation correction reduces the artifactual decrease in activity caused by attenuation, so that the image appearance more accurately represents the actual activity in the myocardium. Thus, attenuation correction leads to improved quantitation, improved image quality, and may lead to improved specificity for myocardial perfusion.

While the attenuation effects seen on many perfusion scans can be interpreted correctly through references to normal images and through training [9], correction of the attenuation artifacts caused by variation between patients may improve the specificity of the imaging technique [4]. The Optima NX provides attenuation correction with little effect on patient throughput, scan time, and patient dose.

*Improved  
Quantification*



## TRANSMISSION SCANNING

In order to correct for attenuation in the thorax, the shape and attenuation of the organs in the thoracic cavity must be known. The lungs, breast tissue, and myocardium are significantly different in their attenuation.

The attenuation is measured by detecting the photons from a transmission source that travel through a patient. The transmission source is done at a range of angles, using an acquisition similar to that for a step and shoot SPECT acquisition. This data is reconstructed to obtain the attenuation coefficients in the transaxial sections.

The Optima NX system provides the most efficient way of acquiring 180° cardiac SPECT data with its two detectors at 90° orientation. The dual transmission source design [5, 6, 7] allows a similar acquisition of the transmission data (Figure 1).

### Transmission Scan Hardware

On the Optima NX, a long lived collimated rod source of Gadolinium-153 (Gd-153) is used. Gd-153 has a half life of 242 days with an emission energy of 100 keV. The source is solid sealed and has an initial activity of 18.5 GBq (500 mCi). To reduce patient exposure from the low energy (41 keV - 49 keV) gamma rays, a 0.5 mm thick copper strip is permanently fixed to the collimator aperture. An additional 2 mm thick copper filter reduces the effective activity to 9.25 GBq (250 mCi) for scanning purposes. After approximately one half life, the filter strip is removed. This allows the full strength of the remaining activity to be used for an additional half life, thus extending the useful life of the source.

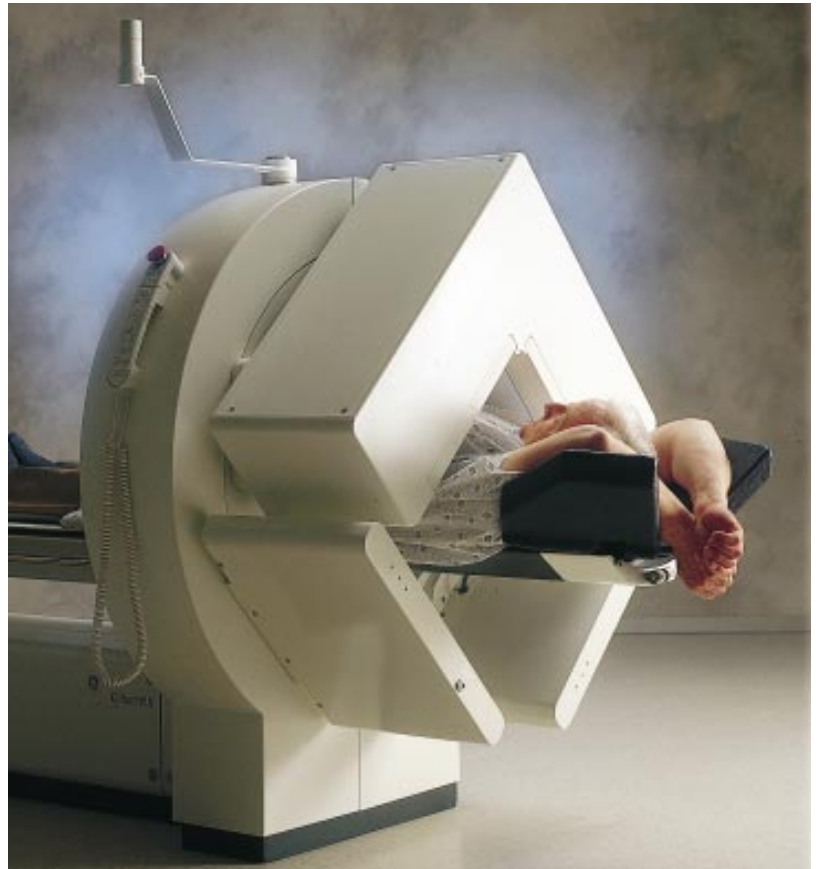
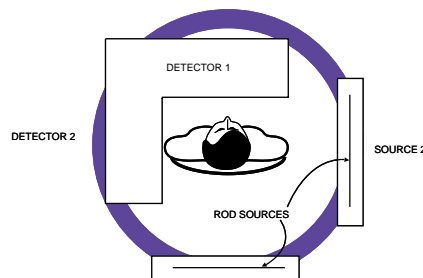


Figure 1: Optima NX

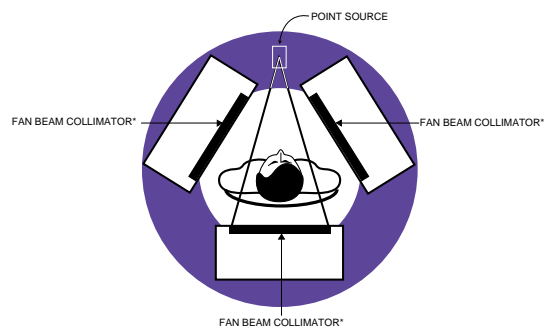
The Gd-153 source is contained in a collimated enclosure and is shielded when not in use. The source, collimator, and scanning mechanism are enclosed in a flat scan box, which is mounted on the Optima NX gantry. Two Optima NX transmission scanning drives are permanently installed in the scanning boxes and do not interfere with other imaging exams nor routine operator quality control. The two identical scan boxes are mounted on the gantry opposite each detector, allowing for acquisitions of 180° SPECT data with a 90° gantry rotation. Since the scan boxes are permanently attached to the gantry, the operator does not have to spend time attaching and removing these devices.

With the Optima NX, the transmission and emission scans are performed with the same detector collimators (e.g. LEHR, LEGP) that are already present on the system. There are no additional hardware modifications required regardless of the acquisition type, either *Sequential*, *Simultaneous* or *Simultaneous Interleaved*. (See Transmission/Emission Acquisition for details). Also, there is no need to change to a fan beam collimator [8] as seen with some gamma camera systems (Figure 2).

*Optima two-detector system demonstrating parallel-beam transmission imaging with truncation-free scanning*



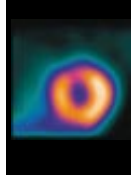
*Three-detector system demonstrating fan-beam transmission scanning*



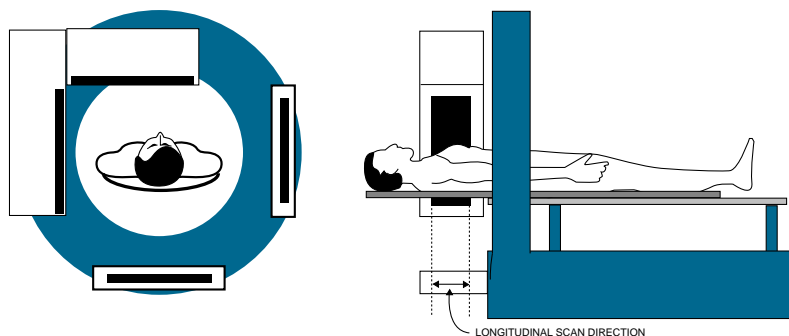
\* NON-STANDARD COLLIMATORS

Figure 2: Comparison of an Optima NX with a Triple Head Camera

# Performance



The transmission source is aligned along the transverse axis and is scanned along the long axis of the patient. The source and its collimator scan are under computer control. A line source within each scan box moves away from the gantry during one transmission acquisition and then towards the gantry on the next acquisition (Figure 3). Beams of 100 keV gamma rays from the two sources pass through the patient and are detected by the two opposing Optima NX detectors.



Transmission Imaging with Dual Scanning Gd-153 Line Sources

Figure 3: Attenuation Correction on the Optima NX

### Transmission Scan Mask

An electronic transmission scan mask is available for all transmission scanning as described below. One of its main purposes is to reduce the crosstalk from the emission scan into the transmission image [9].

- ◆ The width of the transmission mask in the line source (X) direction is the entire detector field of view (Figure 4).

- ◆ The size of the transmission mask in the scanning (Y) direction is adjustable between 20 mm to 80 mm. This size is set in the acquisition templates as a function of the collimator selected.
- ◆ The transmission mask can be either positive or negative. Characteristics of these masks are described in Table 1.

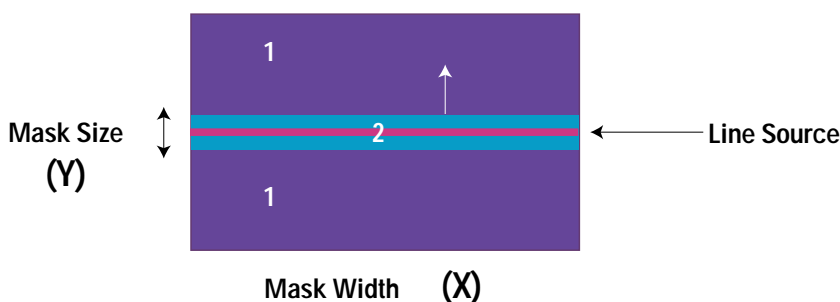


Figure 4: Electronic Masking

Electronic masking in combination with energy discrimination is used to discriminate between transmission and emission events. For example, in Region 1, any 100 keV event detected must be scatter from either the 140 keV technetium peak or the 167 keV thallium peak.

REGION	POSITIVE MASK	NEGATIVE MASK
1 - Counts from patient	Rejected	Accepted
2 - Counts from patient & transmission source	Accepted	Rejected

Table 1: Mask Comparisons

### Transmission Scan Dosimetry

Figure 5 shows dose measurements for a typical 32 stop, 5 second, dual source transmission scan of a thorax phantom. A maximum exposure of 2.88 microSieverts (.288 mRems) was measured at the right posterior surface of the phantom. This position corresponds to the center of the transmission scan arc. A corresponding skin dose is less than 1/6 of a routine chest x-ray.

The patient radiation exposure from the injected radiopharmaceutical used for the emission scan is much greater than from the transmission scan even though the activity injected into the patient is much less than the activity of Gadolinium-153. This is because the radiopharmaceutical can remain in critical organs for many hours subjecting the patient to a continuous exposure as the radioisotope decays or is cleared from the body. For example, the exposure to the kidneys from a thallium injection is estimated at 2 Rads per mCi or 20 mGy per 37 MBq [10].

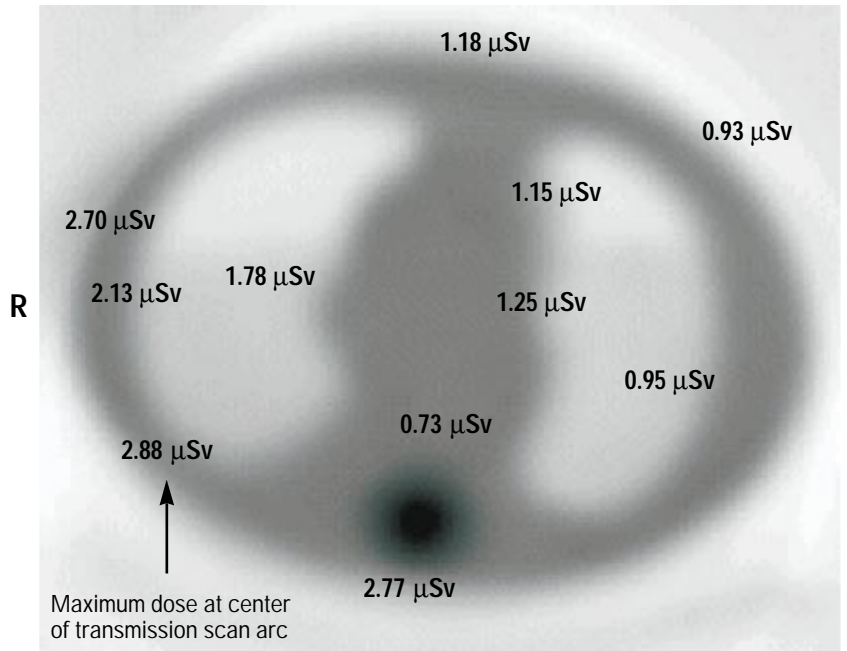


Figure 5: Radiation Exposure in microSieverts

When the sources are “parked” (not scanning), there is no significant radiation leakage from the scan boxes. The dose rate, 1 meter from the box is less than 1 microSievert/hr (0.1 mRem/hr) and is less than 2 microSieverts/hr (0.2 mRem/hr) at the surface of the box.

When the source is scanning, the collimation directs the radiation toward the detector as indicated by the solid arrows (Figure 6). However, some radiation will appear around the edge of the detector as indicated by the longer solid arrow. There is no significant radiation emanating from the back of the scan box as indicated by the dashed arrows.

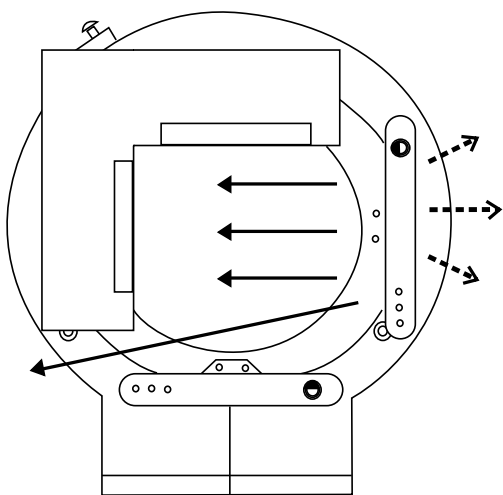
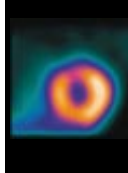


Figure 6: Radiation leakage from a scan box



## TRANSMISSION/EMISSION ACQUISITIONS

The main types of scan data acquired for attenuation correction are the emission and transmission images:

- ◆ Emission images contain gamma rays emitted from the radiopharmaceutical injected into the patient.
- ◆ Transmission images contain the 100 keV photons emitted by the rod source as transmitted through the patient. When a transmission scan is performed on a patient already injected with the radiopharmaceutical, it is possible to acquire both the emission and transmission data into separate image sets.

Additional images are acquired to correct for “crosstalk” and scatter:

- ◆ Crosstalk data contains photons that have spilled down from the 140 keV window (for technetium) into the 100 keV window. Crosstalk is acquired with the transmission source parked and is used to estimate the emission scatter into the transmission window.
- ◆ Scatter data contains scattered photons that have been detected from within the patient. (See Tables 4 and 5 for more details).

The tomographic data can be acquired in three ways:

- ◆ *Sequential* acquisitions, where a separate tomographic scan is performed for each emission and transmission scan.
- ◆ *Simultaneous* acquisitions, where both the emission and transmission images are acquired at the same time per view and in one tomographic rotation [11].
- ◆ *Simultaneous Interleaved* acquisitions, where both the emission and transmission images are acquired sequentially per each view and in one tomographic rotation.

Each of the three methods have distinct advantages and disadvantages. These are listed in Table 2. The main advantage of the Sequential method is uncontaminated emission data. The standard protocol used for non-attenuation corrected data can be used for the emission acquisition. It does have major drawbacks of taking a longer time to complete and photon registration in situations with patient motion, cardiac creep, and movement of internal organs between the emission and transmission scans.

Simultaneous transmission and emission scanning virtually eliminate any problems of patient motion or cardiac movement/creep in the thorax [12]. However, there is some scatter or cross-contamination between the emission and transmission data. Since the acquisition parameters, such as time per view, must be the same for both the emission and transmission scans with the Simultaneous method, there may be some modifications required for the emission protocol. Furthermore, gated imaging cannot be performed

Simultaneous Interleaved acquisition combines the advantages of the previous method while avoiding the disadvantages. With this type of acquisition, the emission scan is acquired typically for 20 seconds followed immediately by a 5 second transmission scan for each tomographic view.

*The Optima NX hardware is able to perform Sequential and Simultaneous Interleaved methods using multiple energy acquisitions and electronic masking to acquire the transmission and emission data into separate images.*

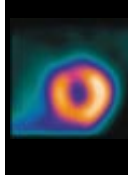
METHOD	ADVANTAGES	DISADVANTAGES
Sequential	Uncontaminated emission data	Timing: two separate acquisitions
	Gated acquisitions	Photon registration between acquisitions: (patient motion)
Simultaneous	Timing: one acquisition	Emission contamination with transmission data
Simultaneous Interleaved	Photon registration occurs at the same time	No gated acquisitions
	Timing: one acquisition	
	Photon registration occurs at the same time	
	Uncontaminated emission data	
	Gated acquisitions	

Table 2: Acquisition Method Comparisons

### Sequential Emission/Transmission Scanning

The Sequential acquisition requires separate emission and transmission scans. For the Optima NX, two 90 degree rotations are required. The emission scan can be either a gated or non-gated acquisition. The acquisition parameters are the same for both scans, except for the radionuclide dependent parameters and the scan time. Depending upon the procedure and radiopharmaceutical, the emission tomographic scan is set (e.g. 20 sec/stop).

The transmission tomographic scan is set for 5 sec/stop. It has been found that a transmission scan time of 5 sec per stop is sufficient, even for obese patients [2].



### Simultaneous Interleaved Emission/Transmission Scanning

The Simultaneous Interleaved acquisition permits the acquisition of the same type of data as obtained in Sequential emission/transmission scanning. However, the emission and transmission scans are both performed sequentially in one view at a time. The Simultaneous Interleaved method is faster than the Sequential because only one rotation is required. The data collection scheme is illustrated in Table 3 and shows the acquisition data in two phases for each view. All the acquisitions have the same image parameters such as matrix size, zoom, etc., and the two phases use the same energy set definitions, denoted as ES1 through ES4 in the table. (Note: Although the emission acquisition can be either

gated or non-gated, Table 3 provides information on non-gated imaging data.)

During each time period, data is acquired into all of the energy sets. The acquisition time for each view is divided into two parts:

- ◆ The first part occurs when the transmission source is off and the emission, crosstalk, and scatter data are being acquired. No scan mask definitions are applicable since the source is off.
- ◆ The second part occurs when the source is scanning and transmission, emission and scatter data are being acquired. The scan mask defined for each set (positive, negative, none) is applied during the scanning phase. (See the section on Transmission Scan Mask).

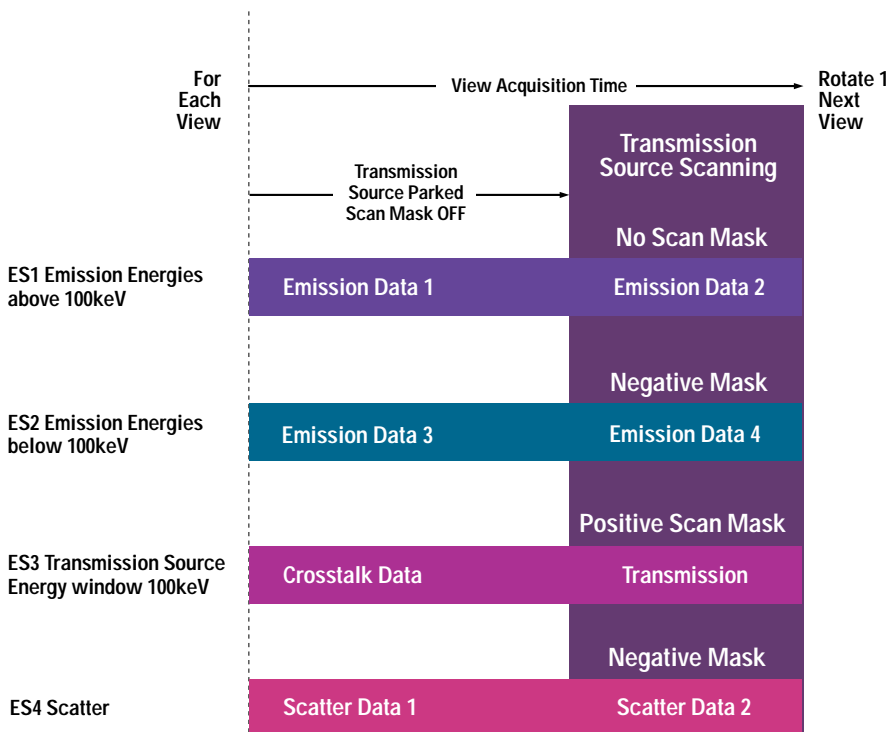


Table 3: Simultaneous Interleaved Emission/Transmission Data Acquisition Scheme

The data is stored in one series containing up to eight non-gated image sets. Each image set is stored as a tomographic data type, which can be individually selected for cine and review.

Depending on the radionuclide used, the acquisition produces different energy sets for processing. The radionuclides, Tc-99m and Tl-201, and their acquisition characteristics are listed in Tables 4 and 5.

On the Optima NX, technetium acquisitions typically use the LEHR collimator, two detectors, 32 stops, a 90 degree rotation and the following energy sessions, which result in six image sets:

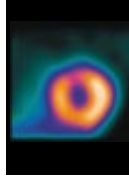
ENERGY SET	SOURCE OFF E SET NAME	SOURCE ON E SET NAME	keV	WIDTH	MASK
1	Emission 1	Emission 2	140	20	None
2	Crosstalk	Transmission	100	20	Positive
3	Scatter 1	Scatter 2	117	12	Negative

Table 4: Technetium Acquisition Energy Sets

Thallium acquisitions usually use the LEGP collimator, two detectors, 16 stops, a 90 degree rotation, and the following energy sessions which will result in eight image sets:

ENERGY SET	SOURCE OFF E SET NAME	SOURCE ON E SET NAME	keV	WIDTH	MASK
1a	Emission 1	Emission 2	167	20	None
1b	Emission 3	Emission 4	72	20	Negative
2	Crosstalk	Transmission	100	20	Positive
3	Scatter 1	Transmission	60	15	Negative

Table 5: Thallium Acquisition Energy Sets



## RECONSTRUCTION METHODS AND ATTENUATION CORRECTION

Reconstruction methods can be grouped into two general classes - direct and iterative. Direct methods, such as Filtered Back Projection, have been used in most SPECT reconstructions. From the standpoint of attenuation correction, no direct method to compensate for non-uniform attenuation exists. Iterative reconstruction algorithms offer much more flexibility and can correct for non-uniform attenuation. Attenuation, scatter and the detector response function can be modeled in iterative reconstruction algorithms, so they are clearly the choice for attenuation correction.

### Attenuation Correction Methods

#### Attenuation Correction With Direct Reconstruction

Direct attenuation correction methods, such as the Sorensen or Chang method [13], apply a correction either to the projections or the reconstruction using Filtered Back Projection. These direct techniques are very fast, but usually require some assumptions to be made about the degree of attenuation and the distribution of activity. For example, the Sorensen method, which is currently available on a GENIE Processing and Review workstation, corrects for attenuation using a body outline derived from fitting an ellipse to the patient outline seen on the emission data [14]. A pre-processing correction is performed assuming a uniform attenuation profile. This approach produces acceptable results in cases where the assumption of uniform attenuation is correct, such as liver and mid brain scans.

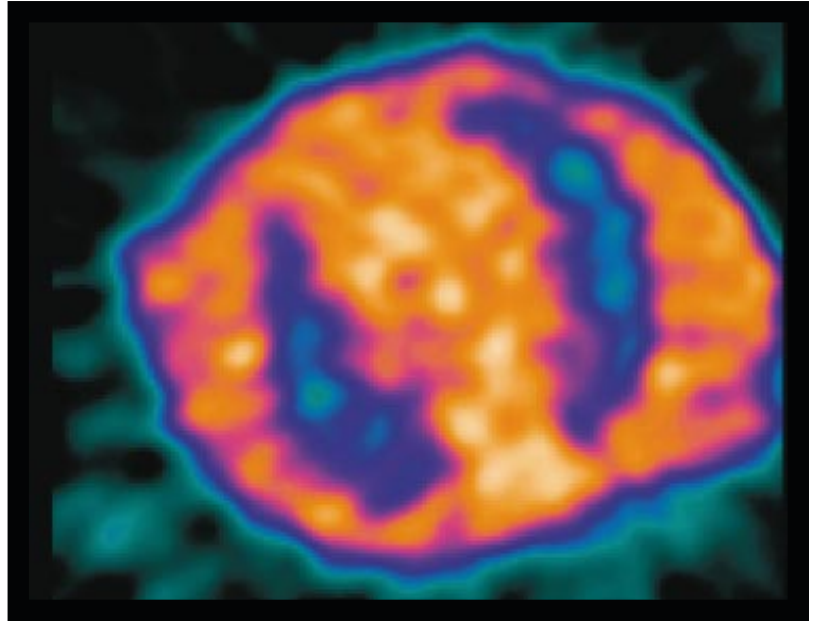


Figure 7: Transmission scan data

#### Measured Attenuation Correction

For measured attenuation correction methods, the attenuation of the patient is determined by using a transmission acquisition, which is then used to generate transaxial maps as discussed in the next section. The maps resemble CT images and provide sufficient information to define the low density lungs and the heart inside the thorax (Figure 7). These maps, along with the emission data, are used to correct for attenuation using an iterative reconstruction method.

#### Attenuation Map Reconstruction

##### Crosstalk Correction

The transmission scan is acquired with a mask to reduce the amount of emission contamination. The remaining emission contamination is measured in a crosstalk image, which acquires the emission contamination using a 100 keV energy window during the emission scan when the source is off. This crosstalk data is scaled to the same acquisition time per pixel as the transmission data, smoothed, and subtracted from the transmission data.

### **Source Flux Correction**

A source profile curve, which is determined once when the source is installed, characterizes any irregularities in the transmission source. The source profile curve is then used along with a standard blank scan to calculate how the blank would appear at the same radius at which the patient was acquired. This normalized blank scan is used to correct the transmission data.

The crosstalk corrected transmission image is divided into the normalized blank scan [15] to compute the ratio of the transmission source flux with and without the patient in the camera's field of view. The negative log of the ratio is the attenuation through the patient.

### **Map Reconstruction**

The integral attenuation images are reconstructed by a standard Filtered Back Projection method to produce the attenuation maps. On the GENIE Processing and Review computer, the displayed attenuation maps have pixel values representing the attenuation per cm, multiplied by 1000. For example, a pixel value of 170 represents an attenuation value of 0.17 per cm.

### **Emission Pre-processing**

#### **Attenuation Map Scaling**

The attenuation map represents patient attenuation as measured at 100 keV. For use in iterative reconstruction, the attenuation values are scaled to the appropriate energy of the emission isotope.

### **Scatter Correction**

The emission data is corrected for scatter by subtracting the suitably scaled, scatter image.

Scatter correction is performed prior to iterative reconstruction using a dual energy window subtraction (DEWS) method [16].

### **Uniformity Correction**

The emission image is then optionally corrected for the collimator uniformity using an acquired uniform flood image. The corrected images are used in the iterative reconstruction process.

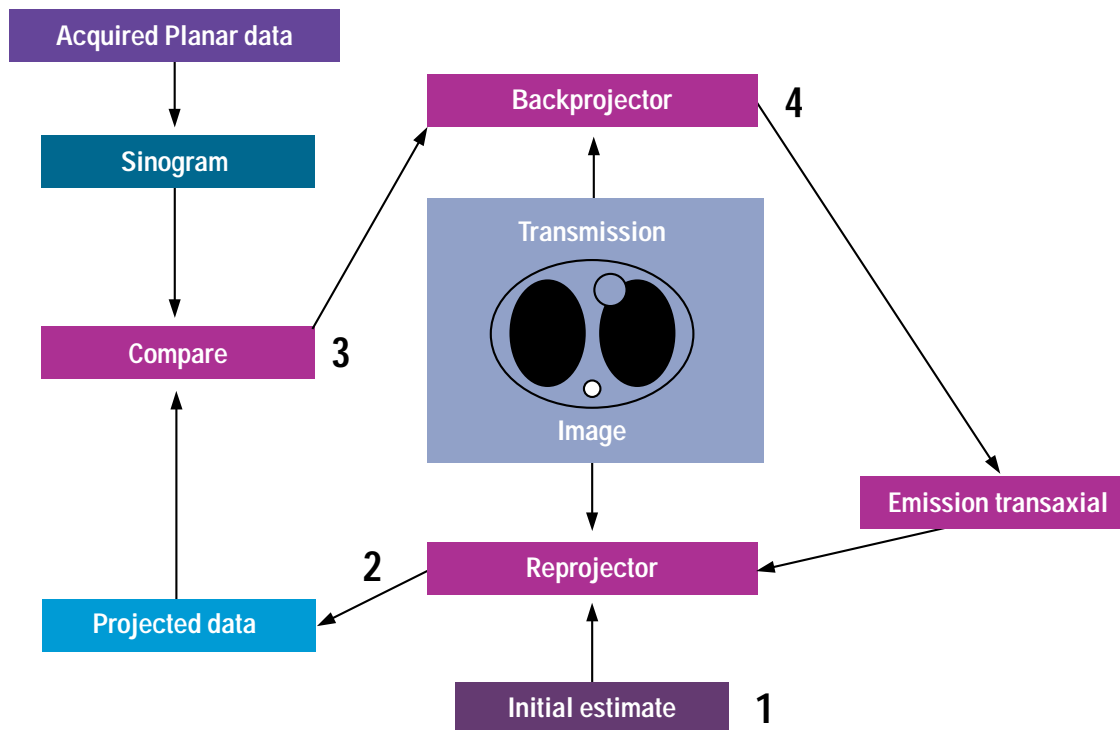


### Iterative Reconstruction Processing

Iterative reconstruction methods can provide more quantitative imaging information and incorporate the effects of noise, counting statistics, missing data and attenuation. In myocardial perfusion imaging, iterative reconstruction reduces the false positive rate caused by scatter, depth dependent detector responses (resolution), and attenuation from the myocardium, breast and diaphragm.

A typical iterative algorithm [17, 18] uses the planar data (projections) and produces images according to the following steps (Figure 8):

1. An initial estimate of the transaxial distribution is created, which may have the total acquired counts uniformly distributed, or which may be a closer guess from another reconstruction process such as Filtered Back Projection.
2. Projections are created from the current estimate by correcting for the actual attenuation taken from the attenuation maps.
3. The difference between the simulated projections and the actual projection is computed, and the estimate of the image is updated.
4. Steps 2 and 3 are repeated a number of times, or iterations, until the pre-defined termination criteria are met.



## Iterative Reconstruction Algorithms

Two iterative reconstruction methods, used on a GENIE Processing and Review workstation, are Ordered Subsets Expectation Maximization (OSEM) and Maximum Likelihood Expectation Maximization (MLEM).

### OSEM

The OSEM method divides the full set of views into subsets. The computer then updates the image using one subset at a time until all views have been used. In the GENIE Processing and Review computer, each pair of subsets consists of two orthogonal views. In the case of 64 images, 32 pairs of views are used to complete one iteration (Figure 10). OSEM is much faster than MLEM since two OSEM iterations produce results comparable to the 20 - 30 iterations of MLEM.

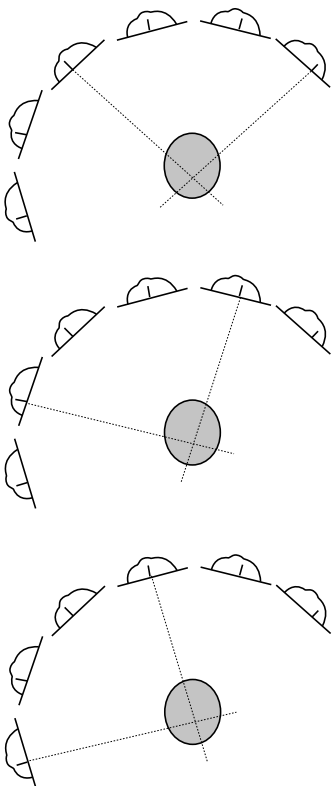


Figure 10: OSEM Method of Iterative Reconstruction [21]

### MLEM

The conventional MLEM method updates the image using all projections in each iteration. In the case of 64 projections, all 64 image frames are used for each iteration. Typically 20 - 30 iterations are required to achieve a satisfactory image (Figure 9).

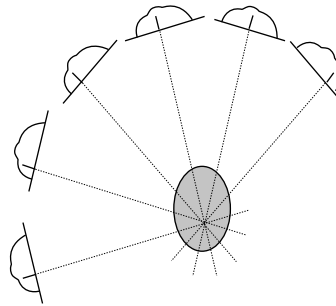
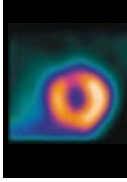


Figure 9: MLEM Method of Iterative Reconstruction [19, 20]

### Emission Post-processing

Emission post-processing involves the application of a filter after the data has been reconstructed. A three dimensional Hanning or Butterworth filter is applied to the emission transaxial slices following iterative reconstruction. If the post filter is changed, only the final post-processing step needs to be repeated. It is not necessary to repeat the entire iterative reconstruction process.



## ADDITIONAL CONSIDERATIONS

### Reconstruction Time of Iterative Algorithms

The amount of computation for one iteration is greater than that of a reconstruction method such as Filtered Back Projection. For some techniques such as the Maximum Likelihood (MLEM) technique, upwards of 20 - 30 iterations are needed to achieve a reasonable result. Based on computational load alone, MLEM would result in reconstructions much longer than Filtered Back Projection. However, the Ordered Subset (OSEM) technique is significantly faster than MLEM, since only two iterations are required. Given the increased power of modern workstations and the speed improvements using OSEM, attenuation correction can now be done in a clinically acceptable time. For example, on a GENIE Processing and Review workstation, 16 slices (64 x 64 matrix data) using OSEM require 20 seconds, which include all pre-processing, reconstruction and post-processing.

### Other Iterative Attenuation Methods

Many different iterative attenuation correction schemes have been proposed for emission tomography, and there are many publications describing the methods. Gullberg implemented a number of iterative algorithms and compared them [22], including iterative convolution [17], iterative Chang [12], conjugate gradient [23] and Maximum Likelihood [24]. In common with other works, he found that the fast iterative methods such as the iterative convolution and the iterative Chang gave increased noise. Although the Maximum Likelihood method gave a smoother reconstruction, he indicated that it required many more iterations.

### Limitations of Iterative Reconstruction

The ultimate accuracy of the iterative reconstruction is limited by:

- ◆ The accuracy of the physical model of attenuation, scatter and resolution
- ◆ The accuracy of the acquired data used to estimate the scatter and attenuation in the patient
- ◆ The accuracy (lack of noise) of the emission data
- ◆ The amount of patient motion during acquisition

The reconstruction algorithm is ultimately limited by the quality of the data acquired, so there is still a need for good customer quality control procedures, both for the camera performance and for checking the quality of the acquired patient data.

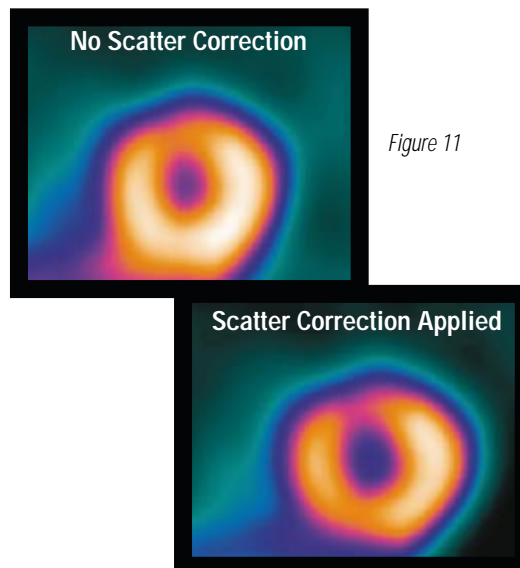
## RESULT

The initial results with attenuation corrected images are encouraging. Attenuation correction has shown to have an impact on the diagnostic accuracy in the inferoposterior wall using Tc-99m tetrofosmin [25]. From attenuation correction studies done on patients injected with thallium-201 [26], there was a more uniform distribution of activity in the myocardium from one patient to another than with standard Filtered Back Projection (FBP) methods. It was concluded that the uptake patterns for men and women are more similar with attenuation correction than with FBP. In addition to a more uniform activity, the studies indicated that there was a decrease in apical activity. Thus, new distribution patterns of myocardial activity emerge with attenuation correction techniques and differ from the familiar patterns of data not corrected for attenuation.

When reviewing images, it is important to define both the normal and abnormal image patterns for attenuation corrected data. When using technetium based radiopharmaceuticals, liver and gastrointestinal activity reduces image quality. Also, it is important to recognize typical artifactual patterns [4] and to develop methods for reviewing acquired data for problems such as patient motion or poor patient positioning techniques.

The results of the tomographic acquisition include a review of the planar data and reconstructed oblique slices of vertical long axis (VLA), horizontal long axis (HLA), and short axis (SA). Many reviewers create polar maps for data review. When analyzing the image data, a variety of comparisons can be made. The comparisons include data recon-

structed by the standard Filtered Back Projection method, iterative reconstruction with and without attenuation correction, and data corrected for scatter correction. Attenuation correction data using iterative reconstruction (OSEM method) with scatter correction shows improved uniform myocardial distribution (Figure 11). The increased counts from liver activity in the inferior and inferoseptal walls are reduced due to scatter correction.



There is some skepticism regarding the value of attenuation correction [27]. Although the actual clinical value of attenuation correction has not yet been completely realized, studies do indicate its value [2, 26, 28]. The ability to interpret image data using attenuation continues to improve based on artifact identification and familiarization with the image data. Employing more sophisticated techniques of Simultaneous Interleaved acquisitions, motion correction, and scatter correction contributes to providing more accurate diagnoses.

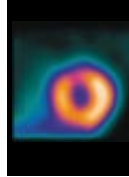
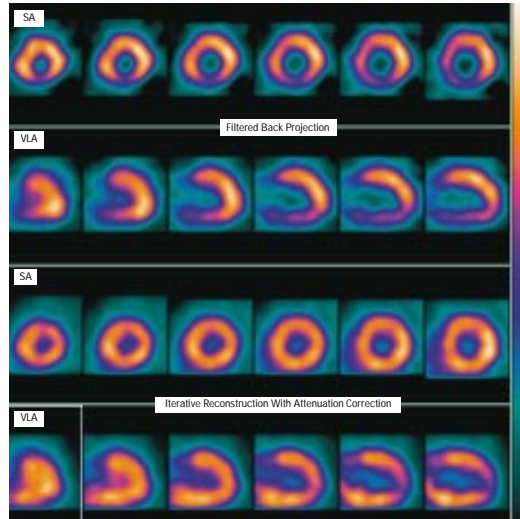
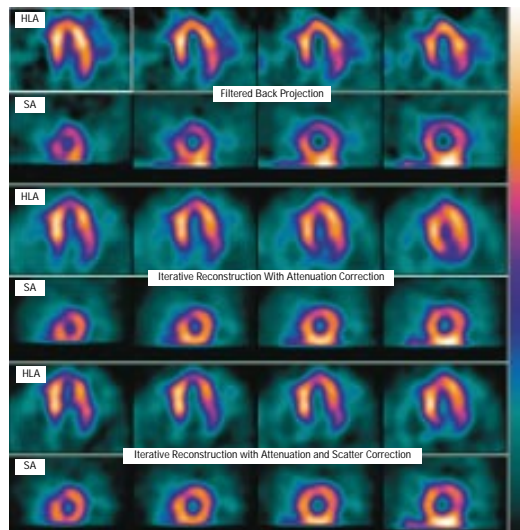
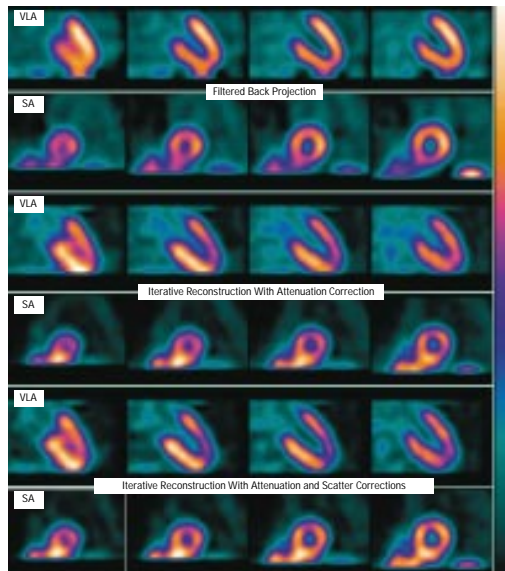


## IMAGE DATA



*Thallium  
Attenuation correction  
data shows improved  
inferior wall uptake*

*TC-99m Sestamibi  
Attenuation correction  
data shows improved  
inferior wall due to  
diaphragm attenuation*



*TC-99m Sestamibi  
Attenuation correction  
data shows improved  
anterior wall due to  
breast attenuation*

## REFERENCES

1. **Tsui BMW, Gullberg GT, Edgerton ER, Ballard JG, Perry JR, McCartney WH, Berg J**, Correction of non-uniform attenuation of cardiac SPECT imaging, *J Nucl Med* 30: 497 - 507, 1989.
2. **Prvulovich E., Lonn AHR, Bomanji J, Jarritt PH, Eil PJ**, Transmission scanning for attenuation correction of myocardial Tl-201 images in obese patients, *Nuclear Medicine Communications Vol 18 pp 207 - 218, 1997.*
3. **Segall GM, Davis MJ**, Prone versus supine thallium myocardial SPECT: a method to decrease artifactual inferior wall defects, *J Nucl Med* 30: 548 - 555, 1989.
4. **DePuey EG, Garcia EV**, Optimal specificity of thallium -201 SPECT through recognition of imaging artifacts, *J Nucl Med* 30: 441 - 449, 1989.
5. **Tsui BMW, Frey EC, McCartney WH, Lonn AHR, Nowak D, Johnston RE**, A fast sequential SPECT/TCT data acquisition method for accurate attenuation compensation in cardiac SPECT, *J Nucl Med Vol 36 No 5 page 169P (Abstract), May 1995.*
6. **Tsui BMW, Frey EC, Johnston RE, McCartney W.H, Lonn AHR, Nowak D, Lange K**, Design of a collimated scanning line source for fast transmission CT data acquisition , *J Nucl Med Vol 36 No 5 page 40P(Abtract), May 1995.*
7. **Cao Z, Tsui BMW**, Performance characteristics of transmission imaging using a sheet source with parallel hole collimators, *Med Physics* 19(5), Sept/Oct 1992.
8. **Jaszczak RJ, Gilland DR, Hanson, Jang, Greer, Coleman RE**, Fast Transmission CT for determining attenuation maps using a collimated line source, rotatable air-copperlead attenuators and fan-beam collimation, *J Nucl Med* 34:9 pp 1577 - 1586, 1993.
9. **Tan P, Baily DL, Meikle SR, Erberl S, Fulton RR, Hutton BF**, A scanning line source for simultaneous emission and transmission measurements in SPECT, *J Nucl Med* 34: 1752 - 1760, 1993.
10. **Higley B, Smith FW, et al**, Technetium-99m-1,2-bis[bis(2-ethoxyethyl)phosphino] ethane: human biodistribution, dosimetry, and safety of a new myocardial perfusion imaging agent, *J Nucl Med Vol 34 No 1 pp 30 - 38, 1993.*
11. **Frey EC, Tsui BMW, Perry R**, Simultaneous acquisition of emission and transmission data for improved thallium-201 cardiac SPECT using a technetium-99m transmission source, *J Nucl Med* 33 pp 2238 - 2245, 1992.
12. **Freidman J, Van Train K, Maddahi J, et al**, Upward creep of the heart: a frequent source of false positive reversible defects on Tl-201 stress redistribution SPECT, *J Nucl Med*, 27: 899 - 900, 1986.
13. **Chang LT**, A method for attenuation correction in radionuclide computed tomography, *IEEE Trans Nucl Sci Vol NS-25 No. 1, pp 638 - 643, Feb 1978.*
14. **Gullberg GT, Malko JA, Eisner RL**, Boundary determination methods for attenuation correction in SPECT, in Esser P, ed. Emission computed tomography, NY: Society of Nuclear Medicine 8: pp 33 - 45, 1983.

# REFERENCES

15. **Tsui BMW, Johnston RE, McCartney WH, Lonn AHR, Nowak D, Colsher JG**, Uniformity correction and calibration method for transmission CT data obtained from scanning line source, *J Nucl Med Vol 36 No 5 page 173P (Abstract)*, May 1995.
16. **Jaszczak Ronald, Greer Kim L, Floyd Carey E, Harris C Craig, Coleman R Edward**, Improved SPECT quantification using compensation for scatter photons, *J Nucl Med 25: 893 - 900, 1984*.
17. **Walters TE, Simon W, Chesler DA, Correia JA**, Attenuation correction in gamma emission computed tomography, *J Comp Assist Tomogr 5(1) pp 89 - 94, Feb 1981*.
18. **Gullberg GT, Huesman RH, Malko JA, Pelc NJ, Budinger TF.**, An attenuated projector-back projector for iterative SPECT reconstruction, *Phys Med Biol 30 No. 8, pp 799 - 816, 1985*.
19. **Shepp LA, Vardi Y**, Maximum likelihood reconstruction for emission tomography, *IEEE Transactions on Medical Imaging, Vol MI-1 No 2, 1982*.
20. **Lange Kenneth, Carson Richard**, EM reconstruction algorithms for emission and transmission tomography, *J Comp Assist Tomogr, 8(2):306-316, April, 1984*.
21. **Hudson Malcolm H, Larkin Richard S**, Accelerated image reconstruction using ordered subsets of projection data, *IEEE Transactions on Medical Imaging Vol XX No Y, 1994*.
22. **Gullberg GT, Malko JA.**, Attenuation correction for quantitative tomography - different methods, *ASL Tech Note 84 - 60 GEMS, July 1984*.
23. **Budinger TF, Gullberg GT, Huesman RH**, Emission computed tomography, in image reconstruction from projections: implementation and application, **Ed GT Herman, Publ. Springer-Verlag pp 147 - 246, 1979**.
24. **Shepp LA, Vardi V**, Maximum likelihood reconstruction for emission tomography, *J Comp Assisted Tomogr, MI-1: pp 113 - 122, 1982*.
25. **Kluge Regine, Sattler Bernhard, Seese Anita, Knapp Wolfram H**, Attenuation correction by simultaneous emission-transmission myocardial single-photon emission tomography using a technetium-99m-labelled radiotracer: impact on diagnostic accuracy, *Eur. J. Nucl. Med Vol 24, No 9, Sept 1997*.
26. **Prvulovich E., Lonn AHR, Bomanji J, Jarritt PH, Eil PJ**, Effect of attenuation correction on myocardial thallium-201 distribution in patients with low likelihood of coronary artery disease, *Eur J. Nucl Med Vol 24, No 4, April 1997*.
27. **Hutton Brian F**, Cardiac single-photon emission tomography: is attenuation correction enough?, *Eur. J Nucl Med Vol 24, No 7, July 1997*.
28. **McCartney WH, Tsui BMW, Adams KF, Lewis DP, Lalush DS, Bujenovic LS, LaCroix KJ, Johnston RE, Perry JR, Lonn AHR, Maniam S, Culp R**, Clinical evaluation of attenuation and scatter compensation in TI-201 SPECT, *J Nucl Med Vol 37, No 5, page 80P (Abstract) May 1996*.



**GE Medical Systems**

Data subject to change.  
Marketing Communications  
GE Medical Systems S.A.  
RCS Versailles B 315 013 359  
For more information on GE, call toll free numbers: 0 800 00 45 10 in France  
(49) 2233 609 398, fax: (49) 2233 609 225 in Germany  
Internet: <http://www.ge.com>

© Copyright GE Medical Systems

GE Medical Systems - Europe: Paris, France  
Fax: +33 (0) 1 30 70 98 55  
GE Medical Systems - Americas: Milwaukee, USA  
Fax: (1) 414 544 3384  
GE Medical Systems - Asia:  
Tokyo, Japan - Fax: (81) 3-3223-8524  
Singapore - Fax: (65) 291-7006  
Printed in France - 8104-BE